Solute–solute spatial distribution in hydrogen bonding liquids probed with time-dependent intermolecular electron transfer

H. L. Tavernier and M. D. Fayer[a)]
Department of Chemistry, Stanford University, Stanford, California 94305

(Received 13 October 2000; accepted 22 December 2000)

Solute–solute spatial distribution in strongly hydrogen bonding solvents is investigated using photoinduced electron transfer dynamics between rhodamine 3B (R3B) and *N*,*N*-dimethylaniline (DMA) in a series of monoalcohols, polyalcohols, and alcohol mixtures. Fluorescence up-conversion data are presented on electron transfer in ethylene glycol and are compared to data characterizing electron transfer in seven other solvents. The data are analyzed with a detailed statistical mechanical theory that includes a distance-dependent Marcus rate constant, diffusion with the hydrodynamic effect, and solute–solute radial distribution functions. When the standard assumption is made that for low concentration solutes the solute–solute spatial distribution follows that of the solvent's radial distribution function, a single parameter fit to the electronic coupling matrix element results in the same value, independent of solvent, for data from five solvents. However, it is impossible to fit the data from the solvent ethylene glycol using the model based on the solvent radial distribution function. When the assumption that the solute–solute spatial distribution tracks the single molecule solvent radial distribution function is relaxed by using a large ''effective'' solvent diameter to establish the donor–acceptor distance distribution and hydrodynamic effect, excellent fits to the electron transfer data are obtained. The fits give the same parameters for ethylene glycol and two other solvents with high OH/C ratios as the five ''normal'' solvents. The results suggest that the solute–solute (donor–acceptor) spatial distributions in the high OH/C ratio solvents are determined by multiple hydrogen bond solvent ''aggregates'' that inhibit solute molecules from distributing freely among solvent molecules. © *2001 American Institute of Physics.* [DOI: 10.1063/1.1349705]

I. INTRODUCTION

Intermolecular electron transfer in liquid solution offers a unique method for probing local environments on the distance scale of angstroms. Distance distributions of molecules on these distance scales have traditionally been calculated or measured with neutron or x-ray scattering.[1] However, these experimental techniques are not sensitive to relatively low concentration solutes, so it is difficult to determine distributions involving solutes in solution. In addition, it is difficult to find calculations of solute–solute or solute–solvent distribution functions that involve molecules that are not hard spheres. Methods are available for these types of measurements on a larger distance scale. For example, electronic excitation transport (EET) is frequently used to probe the structure of local environments.[2–4] EET can be very useful for probing sizes of micelles or isolated polymer chains.[3,4] However, EET generally occurs over longer distances than electron transfer. The rate of singlet state EET falls off as $1/r^6$, where r is the separation between chromophores. Intermolecular donor–acceptor electron transfer, on the other hand, is much shorter ranged. The rate of electron transfer falls off approximately exponentially with distance on an angstrom distance scale.[5,6] Because electron transfer is much shorter range than excitation transport, it can be used to probe local structure on the distance scale of individual molecules.

Because electron transfer occurs on such a short distance scale, it is very sensitive to the short-range spatial distribution of acceptors about a donor. In addition, electron transfer is highly sensitive to properties of the donor/acceptor molecule(s) and characteristics of the local environment.[7–14] Intermolecular electron transfer in liquids also depends on the distribution of donor–acceptor distances, the rate of molecular diffusion, and donor–acceptor orbital overlap.[15–19] In inhomogeneous media, the dynamics of electron transfer are influenced by the dielectric properties of the various regions of the system and the topology of the system.[10,11,13,14,20] Marcus has described the distance-dependent rate of electron transfer.[7,8,21,22] The rate depends on the distance-dependences of electronic interaction, the reorganization energy, and the free energy change associated with transfer.

If all quantities contributing to the rate constant are specified, then the observables in a photoinduced donor–acceptor electron transfer experiment in liquid solution are determined by the radial distribution function of the acceptors (moderate concentration) about a donor (very low concentration) and by the details of the donor–acceptor diffusion. In normal liquids, the donor–acceptor (solute–solute) distance distribution is expected to track the solvent radial distribution function, $g(r)$.[23] Solute molecules can take up

[a)]Author to whom correspondence should be addressed. Electronic mail: fayer@fayerlab.stanford.edu

TABLE I. Measured experimental parameters.

Solvent	τ (ns)	ϵ_{op}	ϵ_{st}	σ_s (Å)
Acetonitrile	1.45	1.7999	35.9[a]	3.62
Ethanol	2.07	1.8523	24.5	4.14
Propylene glycol	2.80	2.0472	29.2	4.72
58/42 propylene glycol/2-butanol	2.66	2.0073	22.3	4.82[b]
23/77 glycerol/2-butanol	2.60	2.0025	19.3	4.90[b]
41/59 glycerol/ethanol	2.34	2.0070	31.9	4.50[b]
50/50 ethylene glycol/ethanol	2.21	1.9631	32.8	4.24[b]
Ethylene glycol	2.38	2.0452	41.5	4.34

[a]Literature value (Ref. 56).
[b]Average diameter of the mixture's components.

TABLE II. Measured diffusive properties.

Solvent	D_{DMA} (Å^2/ns)	D_{R3B} (Å^2/ns)	D (Å^2/ns) ($D_{DMA}+D_{R3B}$)	η (cP)
Acetonitrile	305	133	438	0.341[a]
Ethanol	182	59.8	242	1.08[a]
Propylene glycol	6.7	1.3[b]	8.0	49.90
58/42 propylene glycol/2-butanol	24.4	4.4[b]	28.8	14.70
23/77 glycerol/2-butanol	28.3	4.5[b]	32.8	14.26
41/59 glycerol/ethanol	19.6	8.6	28.2	15.05
50/50 ethylene glycol/ethanol	37.5	7.8	45.3	11.97
Ethylene glycol	11.2	3.7[b]	14.9	17.45

[a]Literature values (Refs. 56,57).
[b]Calculated values, scaled by viscosity from measured D for ethanol: $D = D_{ethanol} \times \eta_{ethanol} / \eta$.

positions that would otherwise be occupied by solvent molecules. If the solute concentration is not too high, then the solvent determines the overall radial distribution function, and the solutes mimic it. The molecular nature of the solvent also influences the diffusion of donor and acceptor molecules at short distances. For small solute–solute separations, intervening solvent molecules hinder the rate of relative diffusion. This effect, called the hydrodynamic effect, can be included in analysis of electron transfer observables[19] using a distance-dependent diffusion constant, $D(r)$.[24–26] In theoretical calculations of time-dependent photoinduced electron transfer experiments, both the donor–acceptor radial distribution function and the hydrodynamic effect combine to provide information on the influence of the solvent on the solute–solute spatial distribution. If the fundamental electron transfer parameters are known for a particular donor–acceptor pair, electron transfer can be used as a tool to understand the local solvent environment on the distance scale of angstroms.

In this study, time-dependent photoinduced electron transfer between donor and acceptor molecules in liquid solvents is used as a probe of the solute–solute (donor–acceptor) spatial distribution function. Electron transfer experiments between rhodamine 3B (photoexcited hole donor) and *N*,*N*-dimethylaniline (hole acceptor) in ethylene glycol are described, and the data and theoretical analysis are compared to previously reported electron transfer studies on the same donor/acceptor molecules in a series of seven solvents.[27] Recent statistical mechanics theoretical developments have made it possible to include all of the salient physical features of electron transfer in liquids in the calculation of experimental observables.[18,19] The data are analyzed using the distance-dependent Marcus rate constant, diffusion with the hydrodynamic effect, and donor–acceptor (solute–solute) radial distribution functions. When the standard assumption is made that for low concentration solutes the solute–solute radial distribution follows that of the solvent,[23] a single parameter fit to the electronic coupling matrix element results in the same value, independent of solvent, for data from five of eight solvents. However, it is impossible to fit the data from ethylene glycol using the model based on solvent radial distribution function. When a solvent radial distribution function and the solvent size in the hydrodynamic effect are fixed at the size consistent with the size of a single solvent molecule, no adjustment of the other parameters, even those that are known, can bring the theory into accord with the data. If an increased ''effective solvent diameter'' is used to establish the donor–acceptor distance distribution and hydrodynamic effect, then excellent fits to the electron transfer data are obtained. These fits to data from ethylene glycol and two other solvents with high OH/C ratios yield the same parameters as the data from the five solvents that can be fit with a normal solvent size. The results suggest that the solute–solute (donor–acceptor) spatial distributions are determined by multiple hydrogen bonded solvent ''aggregates'' that exclude solute molecules from distributing freely among solvent molecules.

II. EXPERIMENTAL PROCEDURES

Reagent grade ethylene glycol (J. T. Baker) was used as received. Solvent viscosity, dielectric properties, and donor/acceptor diffusion were measured with the same grade of ethylene glycol with minimal exposure to atmosphere. One sample contained only rhodamine 3B perchlorate (R3B, Exciton, ~0.04 mM). Three samples were made with R3B as well as *N*,*N*-dimethylaniline (DMA, Aldrich, packaged under nitrogen), with concentrations varying from 0.1–0.3 M. Data were taken previously with similar samples made with the solvents listed in Tables I–III.[27] Details of sample preparation for these samples are presented elsewhere.[27] Throughout this article, R3B is referred to as the ''donor'' molecule, even though it is a hole donor, to be consistent with other work, in which the donor is the low concentration solute that is photoexcited to initiate the electron transfer process. Correspondingly, DMA is termed the ''acceptor'' even though it is a hole acceptor.

A detailed description of the experimental apparatus has been presented previously.[27] In brief, experiments were performed with ~35 ps pulses from two cavity-dumped dye lasers pumped by a mode-locked, Q-switched Nd:YLF laser. R3B was photoexcited at 572 nm. Steady-state fluorescence measurements were made at the magic angle. Time-dependent fluorescence up-conversion was performed at the magic angle with an 880 nm pulse summed with the fluorescence in an RDP crystal. The excitation pulse was delayed in time. R3B fluorescence lifetimes, τ, are the lifetimes measured in samples containing no acceptors (see Table II).

Diffusion constants and redox potentials have been measured by cyclic voltammetry and are listed in Tables I and II.

TABLE III. Solvent hydrogen bonding properties.

Solvent	Mole % ethylene glycol or glycerol	% of solvent carbons with OH groups
Acetonitrile	0	0
Ethanol	0	50
Propylene glycol	0	67
58/42 propylene glycol/2-butanol	0	48
23/77 glycerol/2-butanol	27	41
41/59 glycerol/ethanol	36	73
50/50 ethylene glycol/ethanol	51	76
Ethylene glycol	100	100

Details have been discussed previously.[27] Measurements for R3B were very difficult, and were only measured in acetonitrile, ethanol, ethanol/ethylene glycol, and glycerol/ethanol. For other solvents, the experimental diffusion constant for R3B in ethanol was multiplied by the ratio of solvent viscosities ($\eta_{\text{ethanol}}/\eta_{\text{other}}$), in accordance with the Stokes–Einstein equation, to determine the R3B diffusion constant in another solvent. Viscosities, reported in Table II, were measured using a series of Cannon Ubbelohde viscometers. Theoretical curves used to fit the data were calculated using the mutual diffusion constant, D, which is the sum of the donor and acceptor diffusion constants (see Table II). Since the acceptor is smaller than the donor, it makes the major contribution to the mutual diffusion constant. Therefore, any errors in the R3B diffusion constants that were obtained using the ratios of solvent viscosities have a small effect on the mutual diffusion constants.

Donor/acceptor redox potentials were measured in acetonitrile by cyclic voltammetry. Details have been outlined previously.[27] For acetonitrile, the difference between DMA oxidation and R3B reduction potentials is $\Delta E^0_{\epsilon_{\text{st}}=35.9} = E^0_{\text{DMA,ox}} - E^0_{\text{R3B,red}} = 1.55 \pm 0.06$ eV.

Static dielectric constants, ϵ_{st}, were measured using a concentric cylinder capacitor. Details have been reported previously.[27] Results are reported in Table I. Table I also lists optical dielectric constants, ϵ_{op}, which are the square of the solvent index of refraction. Indices of refraction were measured with a refractometer.

Hard sphere solvent diameters, σ_s, were determined from molecular models of solvent molecules. The volume of each molecular model was measured, and the diameter of a sphere with the same volume is reported in Table I. R3B and DMA radii of $r_d = 4.12$ Å and $r_a = 2.75$ Å, respectively, were determined in the same manner.

III. THEORY AND DATA ANALYSIS

A. Overview

The foundation of the data analysis is a statistical mechanical theory that averages over all acceptor positions to determine the time-dependent donor excited state survival probability (probability that the donor is still excited at time t after excitation), the experimental observable. A theoretical representation of the observable is built from this foundation by including all the factors that are specific to the experimental system. Figure 1 shows a free energy diagram of an experimental system, with parabolas representing ground state, excited state, and charge transfer state. The specific donor/acceptor molecules and solvent characteristics determine the parabola locations, which in turn determine the free energies that characterize the transfer dynamics. Solvent structure and the nature of diffusion in a particular solvent affect donor–acceptor distances, which play an important role in the overall transfer dynamics.

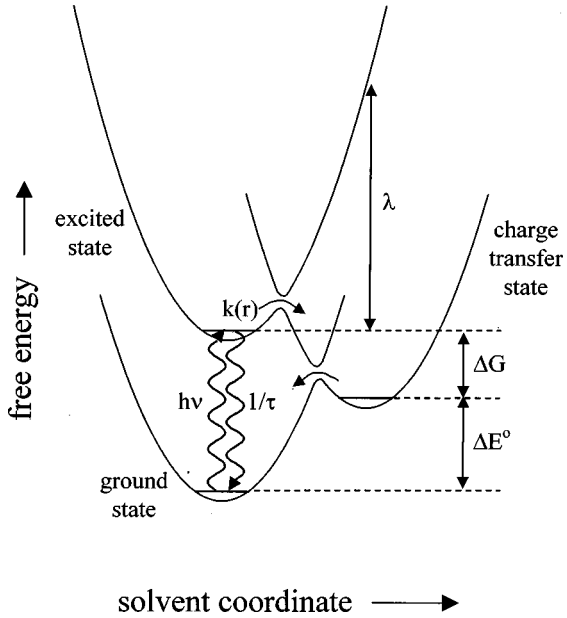

FIG. 1. Free energy diagram representing donor–acceptor ground, excited, and charge-transfer states. The donor is photoexcited with energy $h\nu$. The photoexcited donor either fluoresces with lifetime τ or transfers an electron with rate $k(r)$. The energetics of electron transfer are described by the reorganization energy, λ, the free energy of transfer, ΔG, and the difference between donor/acceptor reduction/oxidation potentials, ΔE^0.

In this article, electron transfer is modeled with a Marcus distance-dependent rate.[7,8,21,22] It has been shown for different solvents and different donor/acceptor systems that intermolecular electron transfer data cannot always be fit with a contact-only or Collins–Kimball rate.[17,27–29] The Marcus rate depends on the magnitude and distance-dependence of donor–acceptor orbital overlap. Because donor–acceptor wave function overlap is nonzero at distances where the molecules are not in contact, it is necessary to include the distance-dependence of the electronic coupling in the distance-dependent rate constant. In addition, the Marcus theory includes the distance-dependent free energy change of transfer and the distance-dependent reorganization energy (ΔG and λ in Fig. 1). Because these terms include Coulomb interactions, they can have substantial distance-dependences independent of orbital overlap factors. It is important to include all factors that influence the distance-dependence of the transfer rate in the data analysis.

Because the rate of transfer depends on distance, the donor–acceptor distance distribution has a significant effect on transfer. It has been shown for hard sphere liquids, and it is presumably true for other models of liquids as well, that with low solute concentrations, the solute spatial distribution

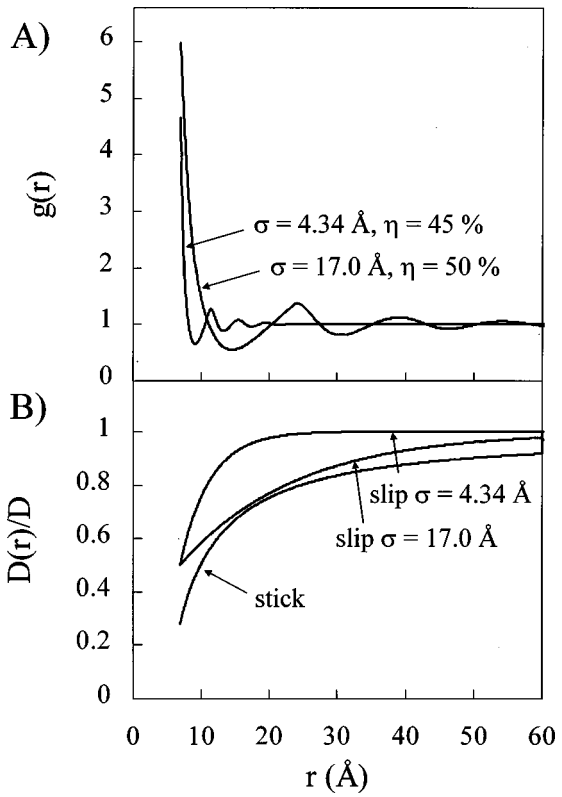

FIG. 2. (A) Hard sphere radial distribution function, $g(r)$, vs. donor–acceptor center-to-center separation distance, r. Hard sphere diameter, σ, determines the oscillation frequency, and packing fraction, η, determines the magnitude at contact. $\sigma=\sigma_s=4.34$ Å and $\eta=45\%$ represents the expected hard sphere $g(r)$ for ethylene glycol. $\sigma=17.0$ Å and $\eta=50\%$ represents the hard sphere $g(r)$ used to fit the ethylene glycol data. $g(r)$ is maximum at the donor–acceptor contact distance, 6.87 Å. (B) Hydrodynamic effect, $D(r)$, for R3B and DMA. The three curves shown are for stick boundary conditions, slip with $\sigma=4.34$ Å, and slip with $\sigma=17.0$ Å. The y values are divided by D so that 1 represents the bulk diffusion constant.

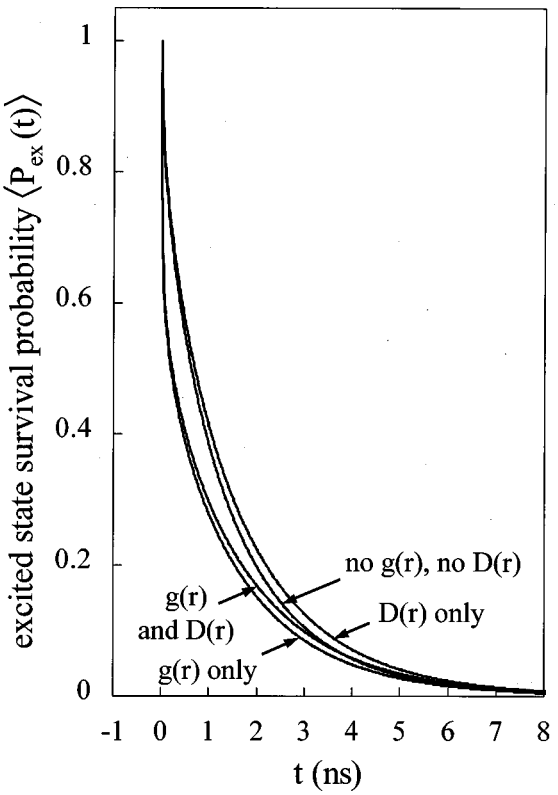

FIG. 3. $\langle P_{ex}(t)\rangle$ decays (the experimental observable without convolution with the instrument response function) demonstrating the effects of donor–acceptor radial distribution function, $g(r)$, and hydrodynamic effect, $D(r)$. Ethylene glycol parameters are used, with [DMA]=0.1 M, $J_0=300\ \mathrm{cm}^{-1}$,and $\beta=1\ \text{Å}^{-1}$. $\sigma=17.0$ Å and $\eta=50\%$ were used for $g(r)$ calculations, and slip boundary conditions with $\sigma=17.0$ Å were used for $D(r)$ calculations. Calculated decays that include $g(r)$ have a very fast short-time component. Decays that include $D(r)$ have a slower long-time component. The curve that includes both $g(r)$ and $D(r)$ is the best fit to the ethylene glycol data.

follows the solvent radial distribution function, $g(r)$.[23] This means that the distribution of acceptor molecules about a donor can be modeled using the solvent $g(r)$. Figure 2(A) shows examples of hard sphere radial distribution functions. Due to solvent packing, molecular density at a separation of one solvent diameter, σ, is appreciably higher than the average density. Correspondingly, finding a molecule 1.5 σ away is less likely than the average probability. Because electron transfer occurs on a short-distance scale and is very sensitive to concentration, the short-distance concentration fluctuations resulting from solvent structure have a major impact on electron transfer observables. As a result, electron transfer is a sensitive probe of local environment on a short-distance scale.

In a liquid, donor–acceptor distances change on the time scales that are relevant for photoinduced electron transfer because of diffusion. In addition to bulk diffusion constants, which can be measured, a distance-dependent diffusion constant must be used to model diffusion properly. When donor and acceptor molecules are near each other, intervening solvent molecules are more likely to block paths of diffusion that bring a donor and acceptor closer together. This results in a distance-dependent diffusion constant, $D(r)$, with diffusion at short donor–acceptor distances being slower than bulk diffusion.[24–26,30,31] Figure 2(B) shows $D(r)$ for stick and slip boundary conditions. For slip boundary conditions, the distance at which $D(r)$ returns to the bulk diffusion constant depends on solvent diameter, σ. Including the so-called hydrodynamic effect in data analysis is important for systems with moderate diffusion constants because electron transfer is occurring to acceptors at distances where $D(r)$ is changing rapidly.

The electron transfer observable, donor excited state population, has a complex, nonexponential time-dependence that can be fit when both $g(r)$ and $D(r)$ are included.[20,27] Figure 3 shows calculated time-dependent donor excited state population with and without $g(r)$ and $D(r)$ for a typical set of electron transfer parameters. Transfer at short times occurs to very nearby acceptors. $g(r)$ increases acceptor concentrations at short distances, causing fast short-time electron transfer. If there are no nearby acceptors, acceptors have to diffuse in toward the donor before electron transfer occurs. $D(r)$ slows the diffusion of these molecules as they approach, ultimately slowing longer-time transfer. While the differences displayed in Fig. 3 are significant, the influence on data analysis increases when data from samples with a range of concentrations of acceptors are fit simultaneously. Only by including both $g(r)$ and $D(r)$ is it possible to theo-

retically fit electron transfer data between R3B and DMA in a variety of solvents.[27]

B. Experimental observables

In the experiments described here, intermolecular electron transfer is initiated by photoexcitation of the donor molecule. Because the donor molecule is in low concentration, the system can be modeled as a single donor molecule surrounded by many acceptors. Both donor and acceptor molecules diffuse in solution. Following excitation, the donor either relaxes to its ground electronic state by fluorescence or nonradiative processes, or undergoes electron transfer to any of a number of nearby acceptors. Electron transfer (in this experiment, donor to acceptor hole transfer) quenches fluorescence. The experimental observables that must be modeled theoretically are time-dependent and steady-state donor fluorescence.

The theory to describe electron transfer in solution has been described in detail and tested previously.[16,19,32,33] Here the necessary results are outlined briefly. The first step in modeling the system theoretically is to describe the one-donor, one-acceptor system. For this two-particle system, $S_{ex}(t|r_0)$ is the survival probability. It represents the probability that the donor is still excited at time t, given that the donor was photoexcited at $t=0$ and that the acceptor was at distance r_0 from the donor at that time. All distances are center-to-center distances. $S_{ex}(t|r_0)$ can be calculated numerically from the following differential equation:

$$\frac{\partial}{\partial t}S_{ex}(t|r_0)=L^{+}_{r_0}S_{ex}(t|r_0)-k(r_0)S_{ex}(t|r_0), \tag{1}$$

where t is time, r_0 is the initial position of the acceptor with respect to the donor, and $k(r)$ is the rate constant of electron transfer at that distance. $L^{+}_{r_0}$ is the adjoint of the Smoluchowski diffusion operator,

$$L^{+}_{r_0}=\frac{1}{r_0^2}\exp\left(\frac{V(r_0)}{k_BT}\right)\frac{\partial}{\partial r_0}D(r_0)r_0^2\exp\left(-\frac{V(r_0)}{k_BT}\right)\frac{\partial}{\partial r_0}, \tag{2}$$

where $D(r)$ is the distance-dependent diffusion constant, k_B is Boltzmann's constant, T is temperature, and $V(r)$ is the distance-dependent potential in which the acceptors are diffusing.

The ensemble averaged excited state survival probability, $\langle P_{ex}(t)\rangle$, can be calculated from employing Eq. (2) in combination with a distance-dependent rate constant, solvent structure, and the hydrodynamic effect. The result is

$$\langle P_{ex}(t)\rangle=\exp\left(-\frac{t}{\tau}\right)\times\exp\left(-4\pi C\int_{r_m}^{\infty}[1-S_{ex}(t|r_0)]r_0^2g(r_0)dr_0\right), \tag{3}$$

where τ is the donor fluorescence lifetime in the absence of acceptors, C is the acceptor concentration, and r_0 is the initial donor–acceptor center-to-center separation distance. $g(r)$ is the solvent radial distribution function used to model the donor–acceptor distance distribution. r_m is the distance of closest approach, the sum of the donor/acceptor hard sphere radii.

In addition to measuring and calculating the time-dependent fluorescence, it is valuable to study the steady-state fluorescence yield, Φ. Because the fluorescence yield is not limited by the time resolution of the time-dependent experiments, it provides some information about electron transfer dynamics on the time scale shorter than the laser pulse length. Φ is the ratio of steady-state fluorescence from a sample with acceptors to one with no acceptors. It can be written using the integrated areas under unconvolved $\langle P_{ex}(t)\rangle$ curves:

$$\Phi=\frac{\int_0^{\infty}\langle P_{ex}(t)\rangle dt}{\tau}, \tag{4}$$

where the area under $\langle P_{ex}(t)\rangle$ with no acceptors is the fluorescence lifetime, τ. For the ethylene glycol experiments presented in this article, a nonnegligible fraction of the electron transfer occurs within the instrument response.

C. Rate constant

$\langle P_{ex}(t)\rangle$ calculations require the distance-dependent rate constant for electron transfer. The rate constant, $k(r)$, involves magnitude and distance-dependent factors including the electronic coupling of the donor to the acceptor, the free energy of transfer, and the reorganization energy. These factors are dependent on donor/acceptor size, orbital overlap, oxidation/reduction potentials, and electronic energy levels as well as solvent dielectric properties.

Marcus has developed a distance-dependent form of $k(r)$ that is well-accepted for nonadiabatic electron transfer in the normal regime ($-\Delta G<\lambda$):[5,7,8,21,22,34]

$$k(r)=\frac{2\pi}{\hbar\sqrt{4\pi\lambda(r)k_BT}}J_0^2\exp\left(\frac{-(\Delta G(r)+\lambda(r))^2}{4\lambda(r)k_BT}\right)\times\exp(-\beta(r-r_m)), \tag{5}$$

where r is the donor–acceptor center-to-center separation distance and $2\pi\hbar$ is Planck's constant. The donor–acceptor electronic coupling terms are divided into J_0, which characterizes the magnitude of coupling at contact, and β, which reflects the exponential distance-dependence of the coupling. Unless other wise specified, $\beta=1$ Å^{-1} was assumed in all calculations because β has been found to be ~ 1 Å^{-1} in many cases.[17,22,29,35,36] In addition, the experiments on R3B and DMA in several solvents (discussed below) were fit successfully taking $\beta=1$ Å^{-1}, and it was found that the fits could not be significantly improved by varying β.[27] The assumption that $\beta=1$ Å^{-1} is tested in the context of the experiments presented here.

The reorganization energy, λ, (see Fig. 1) is composed of both inner sphere (λ_i) and outer sphere (λ_o) components:[22]

$$\lambda=\lambda_i+\lambda_o. \tag{6}$$

The inner sphere reorganization energy, λ_i, is the energy required to modify the molecular structure of the reactant molecules to form the products. In these calculations, it is assumed to be $\lambda_i = 0.10$ eV. For large aromatic organic molecules like rhodamine 3B, values of near 0.05 eV have been calculated for λ_i.[37] To account for both reactants, this value was multiplied by 2. This is within the range of reported λ_i values for organic molecules.[37–40] λ_i is not distance-dependent and is small enough compared to λ_o that it has little effect on the distance-dependence of the rate constant.[27] Its only influence on the theoretical fits to the data is to change the apparent magnitude of electronic coupling.[27] However, because λ_i is solvent-independent, J_0 values resulting from fits can be compared meaningfully if the same λ_i value is used to analyze data for the same donor–acceptor pair in different solvents.

Solvent reorganization energy, λ_o, is the energy required to reorganize the solvent from its reactant-solvating configuration to its product-solvating configuration without actually allowing the electron transfer to occur. A distance-dependent expression for λ_o was derived by Marcus:[7,8,21]

$$\lambda_o(r) = \frac{e^2}{8\pi\epsilon_0}\left(\frac{1}{\epsilon_{\mathrm{op}}} - \frac{1}{\epsilon_{\mathrm{st}}}\right)\left(\frac{1}{r_d} + \frac{1}{r_a} - \frac{2}{r}\right), \tag{7}$$

where e is the charge of an electron, ϵ_0 is the permittivity of free space, ϵ_{op} and ϵ_{st} are the solvent optical and static dielectric constants, and $r_{d/a}$ are the donor/acceptor hard sphere radii.

ΔG, the free energy charge of transfer, is shown in Fig. 1. It depends on excitation energy, redox potentials, and Coulomb interactions. It can be written,[9]

$$\Delta G = \Delta E^0 - h\nu, \tag{8}$$

where $\Delta E^0 > 0$ is the difference between donor/acceptor oxidation/reduction potentials, and $h\nu = 580$ nm is the donor singlet excited state energy, determined by the energy at which normalized absorption and fluorescence spectra cross.[34] This expression is particular to the experimental system used in this work, in which there is no donor–acceptor Coulomb interaction in the reactant or product state. If there were Coulomb interactions, ΔG would be distance-dependent. Redox potentials were measured in acetonitrile ($\epsilon_{\mathrm{st}} = 35.9$). The redox potentials in other similar dielectric constant solvents can be accurately obtained with the following equation:[10,41]

$$\Delta E^0 = \Delta E^0_{\epsilon_{\mathrm{st}}=35.9} + \frac{e}{8\pi\epsilon_0}\left(\frac{1}{\epsilon_{\mathrm{st}}} - \frac{1}{35.9}\right)\left(\frac{1}{r_a} - \frac{1}{r_d}\right). \tag{9}$$

For ethylene glycol, $\lambda(r=0) = 1.16$ eV and $\Delta G = -0.60$ eV. This is well within the normal region of electron transfer ($-\Delta G < \lambda$), as illustrated in Fig. 1. Electron transfer within this regime is described well by the classical form of the electron transfer rate constant given by Eq. (5).[34]

D. Donor–acceptor distance distribution

In the calculations, a hard sphere radial distribution function, $g(r)$, is used to describe the distribution of acceptor molecules about the donor molecules.[23] Calculations that compared results using a hard sphere radial distribution function to a radial distribution function obtained experimentally with neutron scattering showed that the differences were negligible.[20] The donor and acceptor are not in high enough concentration to independently form a structured distribution; under normal circumstances, they tend to follow the structure determined by the solvent molecules.[23] In a hard sphere liquid, the packing fraction, η, is the percent of volume occupied by spherical molecules. Dense, room-temperature liquids generally fall in the range of $\eta = 43\%-48\%$.[23,42–45] In order to pack with this density, spheres create a somewhat ordered system with a radial distribution function that oscillates about the average solvent density of 1 [see Fig. 2(A)]. Normally, oscillations occur with peaks separated by the diameter of the solvent molecules. σ_s will be used to differentiate the single molecule solvent diameter (see Table I) from the diameter σ that is used in $g(r)$ and $D(r)$ in the calculations. Unless otherwise specified, $\sigma = \sigma_s$, and a packing fraction of 45% is used to calculate $g(r)$. However, in some of the calculations $\sigma \neq \sigma_s$. Hard sphere radial distribution functions are calculated by solving the Percus–Yevick equation,[23,46–49] using an algorithm given by Smith and Henderson,[50] and modified by a Verlet–Weis correction.[42]

E. Diffusion

The specifics of diffusion in an experimental system can have a significant impact on the electron transfer dynamics in that system. Two special features of diffusion are included in this theory: the effect of the radial distribution function and the hydrodynamic effect.

Diffusion is affected by the donor–acceptor radial distribution function, $g(r)$, because diffusion must maintain that distribution. Diffusion that maintains $g(r)$ can be included in the theory by requiring the diffusion to occur within a potential of mean force:[1,24,26]

$$V(r) = -k_B T \ln[g(r)], \tag{10}$$

which is included in Eqs. (1)–(2). If a Coulomb interaction between reactants existed, it would also be included in $V(r)$.

The distance-dependent diffusion constant (hydrodynamic effect), $D(r)$[24–26,30,31] can be expressed theoretically with forms that depend on whether stick or slip boundary conditions are appropriate for the particular experimental system. For stick boundary conditions, an expression for $D(r)$ was developed by Deutsch and Felderhof:[25,31]

$$D(r) = D\left[1 - \frac{3r_d r_a}{r(r_d + r_a)}\right], \tag{11}$$

where D is the sum of the donor and acceptor bulk diffusion coefficients and $r_{d/a}$ are donor/acceptor radii. Northrup and Hynes developed a similar expression for slip boundary conditions:[24]

$$D(r) = D\left[1 - \frac{1}{2}\exp\left(\frac{r_m - r}{\sigma}\right)\right], \tag{12}$$

where r_m is the donor–acceptor contact distance, and σ is the solvent diameter.

Figure 2(B) shows the difference between stick and slip forms of $D(r)$. Stick boundary conditions are most appropriate when solute molecules are larger than the solvent molecules, and slip boundary conditions are most appropriate when solute and solvent molecules are similar in size or the solute is small compared to the solvent.[26] Both R3B and DMA are larger than all of the solvent molecules used in this work and in the previous experiments that are discussed in this article (acetonitrile and small alcohols/diols/triols).[27] This would suggest that stick boundary conditions should be used. However, it has been shown experimentally that for rotational diffusion of rhodamine B, stick boundary conditions are most appropriate in monoalcohol solvents and slip boundary conditions are most appropriate in ethylene glycol, glycerol, and ethylene glycol/glycerol mixtures.[51] Although ethylene glycol and glycerol molecules are not necessarily larger than the monoalcohols, slip boundary conditions were justified because the polyalcohols can form hydrogen-bonding networks, effectively behaving like polymers that are much larger than the rhodamine B molecules.[45,51,52] Unless otherwise specified, stick boundary conditions have been used. The application of slip boundary conditions to ethylene glycol and glycerol containing solvents is discussed in Secs. V and VI.

IV. AGREEMENT BETWEEN THEORY AND EXPERIMENT IN SOME SOLVENTS

In a previous article, data were presented on electron transfer between R3B and DMA in a number of liquids.[27] Figures 4–6 show data and fits for electron transfer in three of the liquids: acetonitrile, ethanol, and propylene glycol. Data and fits for two of the other liquids (not shown) yield the same type of results. The data taken in five solvents could all be fit using one adjustable parameter, J_0, the magnitude of the electronic coupling at contact. Figures 4–6 show the quality of the fits to the time-dependent data and the fluorescence yield data. In fitting the data, the measured values of diffusion constants and dielectric constants (see Tables I and II) were used, $\beta=1$ Å^{-1} was fixed, and the radial distribution function employed solvents molecular diameters, σ_s (see Table I).

J_0 should be independent of the solvent; it is a constant that depends on the properties of the donor and acceptor. The important result is that, within experimental error, the fits to the data taken in the five liquids gave the same value of J_0, that is, $J_0=300\pm20\,\mathrm{cm}^{-1}$. This is a remarkable result given the complexity of the systems being studied. It means that the theory is able to separate out the effects of diffusion, donor–acceptor distance distributions, solvent reorganization, and electronic coupling. The exact value of J_0 is less important than the fact that the same J_0 is obtained for each donor/acceptor–solvent system. As discussed previously, the value of J_0 will vary depending on the choice of λ_i, but regardless of the choice of λ_i, all five J_0 are the same.[27] The five solvents have different solvent diameters, diffusion constants, and dielectric properties. When factors like a distance-dependent rate, solvent structure, and hydrodynamic effects were not included, it was not possible to fit the data. But when they are included, it is possible to systematically describe electron transfer in these systems.

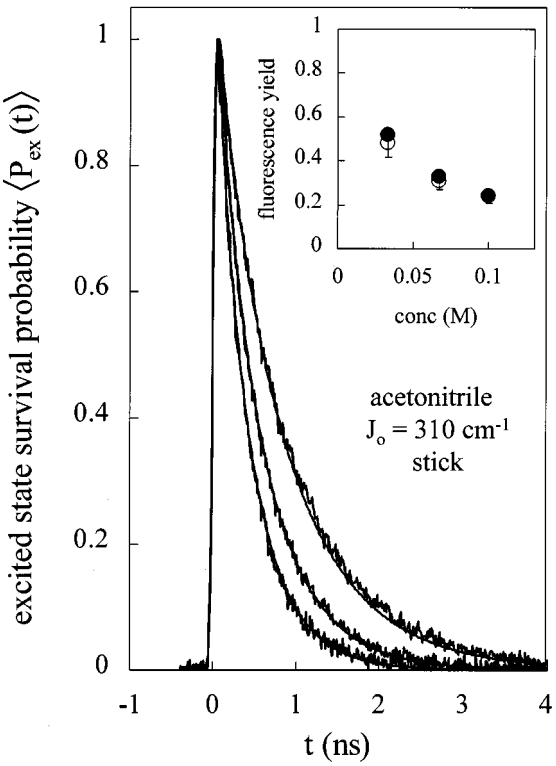

FIG. 4. R3B fluorescence data and fits for three concentrations of DMA in acetonitrile. Inset shows fluorescence yield data (open circles) and fits (filled circles). Calculated curves are the result of a single parameter fit to J_0 resulting in $J_0=310\,\mathrm{cm}^{-1}$.

V. RESULTS IN THE SOLVENT ETHYLENE GLYCOL

Time-dependent and steady-state fluorescence data on electron transfer between R3B and DMA in ethylene glycol are shown in Fig. 7. The data has an appearance that is very similar to the data shown in Figs. 4–6. However, the results of comparing theory to experiment are vastly different than in the cases of the five liquids discussed above.

Calculations were performed in a manner that was identical to the successful calculations on other liquids using the measured diffusion constant, dielectric constants, and solvent diameter shown in Tables I and II with $J_0=300\,\mathrm{cm}^{-1}$ as determined by the previous experiments. It is impossible to fit the data with these parameters. It is impossible to fit the data with these parameters even if the electronic coupling parameters, J_0 and β, are allowed to vary. Figure 7 shows the best fits possible by fitting both to J_0 and β. For $J_0 \geqslant 700\,\mathrm{cm}^{-1}$ there are many different pairs of J_0 and β that give comparable fits, with β increasing as J_0 increases. Any J_0/β pairs that do a better job fitting the time data give much worse fits to the yield, and vice versa. It is possible to fit the time moderately well by varying both J_0 and β, *but the yield calculations are up to 360% different from the experimental values.* Even with the poor quality of time fits shown in Fig. 7, the yield calculations are off by up to 180%. Two parameter J_0/β fits are shown for stick boundary conditions because with the ethylene glycol diameter of 4.34 Å, fits to the

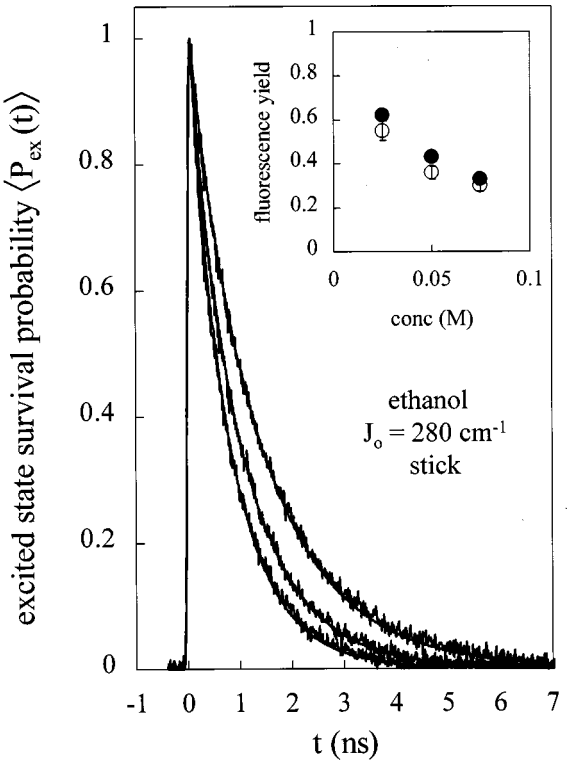

FIG. 5. R3B fluorescence data and fits for three concentrations of DMA in ethanol. Inset shows fluorescence yield data (open circles) and fits (filled circles). Calculated curves are the result of a single parameter fit to J_0 resulting in $J_0=280\ \mathrm{cm}^{-1}$.

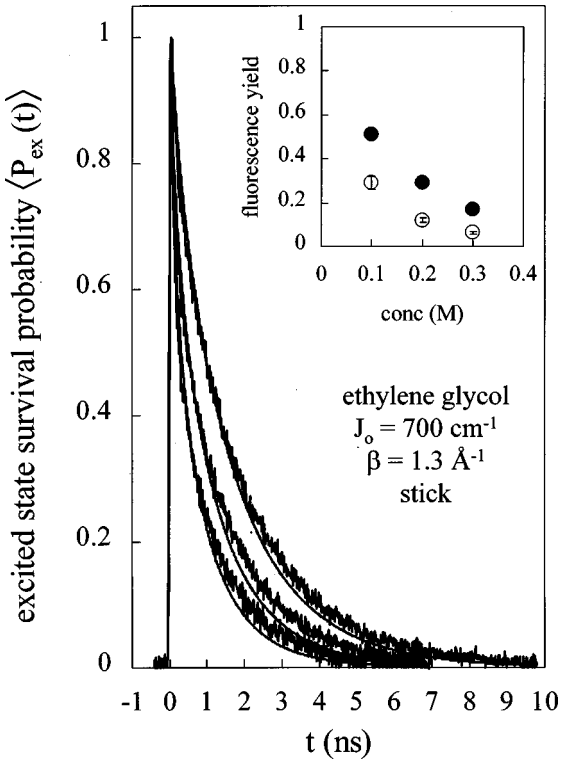

FIG. 7. R3B fluorescence data and fits for three concentrations of DMA in ethylene glycol. Inset shows fluorescence yield data (open circles) and fits (filled circles). Calculated curves are the result of two-parameter fits to J_0 and β, with ethylene glycol parameters and stick boundary conditions. $J_0=700\ \mathrm{cm}^{-1}$ and $\beta=1.3\ \mathrm{Å}^{-1}$. Fits to both time and yield are poor. It is not possible to obtain better fits to the ethylene glycol data if other system parameters are not allowed to vary.

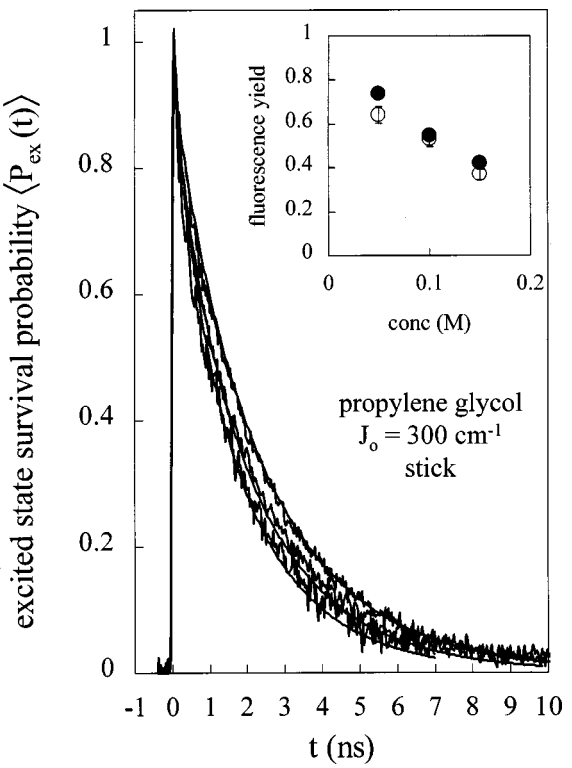

FIG. 6. R3B fluorescence data and fits for three concentrations of DMA in propylene glycol. Inset shows fluorescence yield data (open circles) and fits (filled circles). Calculated curves are the result of a single parameter fit to J_0 resulting in $J_0=300\ \mathrm{cm}^{-1}$.

data with slip boundary conditions are notably worse. Ultimately, it is impossible to fit the ethylene glycol data by changing only the electronic coupling parameters.

The fluorescence yield data shows an anomalously large amount of transfer. For comparable concentrations, the fluorescence yield in ethylene glycol is similar to the yield in significantly less viscous solvents like acetonitrile and ethanol. The low yield in acetonitrile and ethanol is due to the fast diffusion in those solvents. There is much less transfer in any of the other solvents. When all of the other parameters are fixed ($J_0\sim 300\ \mathrm{cm}^{-1}$), the low yield in ethylene glycol can only be accounted for by requiring fairly extreme parameter values of either $J_0>1200\ \mathrm{cm}^{-1}$, $\beta<0.5\ \mathrm{Å}^{-1}$, or $D>80\ \mathrm{Å}^2/\mathrm{ns}$. Each of these parameter choices increases the overall amount of transfer in the calculation and makes it possible to fit the yield data. However, if the yield is fit by one of these parameter choices, the time-dependent calculations are very poor in comparison to the data.

The time-dependent data for ethylene glycol has a somewhat unusual shape, and is even more difficult to fit than the yield data. It has a very fast short-time component combined with a fairly slow longer-time component. With all other parameters fixed, the only way to get good fits to the time data are to fit with $J_0>1000\ \mathrm{cm}^{-1}$ in combination with $D<4\ \mathrm{Å}^2/\mathrm{ns}$. A large J_0 effectively models the fast short-time component by causing a large amount of transfer to acceptors that are initially nearby. The small diffusion constant

brings more acceptors in slowly, allowing the calculations to fit the slower long-time behavior. None of the fits to the data give accurate fits to the yield data. The only way to simultaneously fit time and yield data is using $J_0=2100\,\mathrm{cm}^{-1}$, $D=1.0\,\text{Å}^2/\mathrm{ns}$, and assume slip boundary conditions.

Although it is possible to fit ethylene glycol time and yield data with very large J_0 and small D, these values are not physically reasonable. $D=14.9\,\text{Å}^2/\mathrm{ns}$ was measured experimentally by cyclic voltammetry.[27] This value agrees perfectly with the value of D predicted by scaling the measured D for ethanol by viscosity ($D=D_{\mathrm{ethanol}}\times\eta_{\mathrm{ethanol}}/\eta$) in accordance with the Stokes–Einstein equation. There is no reason to believe that the measured value of D could be off by a factor of 15. It is also reasonable to take the value of $J_0=300\,\mathrm{cm}^{-1}$ which was shown to characterize transfer between R3B and DMA in five different liquids.[27] The largest source of error in J_0 is the choice of λ_i, but λ_i is an internal molecular parameter, and it is independent of solvent. Therefore, changing the value of λ_i changes the value of J_0 uniformly in all solvents. In addition to being experimentally reproduced in five liquids, 300 cm^{-1} is within the expected range of J_0 values.[5,17] The choice of β and boundary conditions are justified and do not substantially affect the resulting fits. If $\beta=1.0\ \text{Å}^{-1}$ is changed by $\pm0.2\ \text{Å}^{-1}$, either the time or the yield data fit worse, so $\beta=1.0\ \text{Å}^{-1}$ is the appropriate value.

In addition to varying all of the relevant parameters in attempts to fit the data in ethylene glycol, other explanations for the lack of agreement between theory and experiment were considered. The possibility that the DMA aggregates around the R3B was investigated. Absorption spectra of R3B were taken as a function of DMA concentration, with [DMA] ranging from zero concentration to the highest experimental DMA concentration. No changes were observed that would suggest specific aggregation. To further test the possibility that aggregating is responsible for the form of the data, calculations were performed that included acceptor aggregation about the donor. To model acceptor aggregation, the radial distribution function was modified by increasing the first peak (the peak representing the first shell about the R3B) in height while keeping the total radial distribution function normalized. In addition, lower bulk DMA concentrations were tried, to account for decreased available concentration resulting from aggregation. Increasing the first peak placed more DMA molecules close to the R3B than would occur without a specific attractive interaction between donor and acceptor. The increased local concentration caused the short-time portion of the decays to become faster, but the shapes of the curves and the yield calculations were not consistent with the data for any possible DMA concentrations, regardless of the height of the first peak in the radial distribution function. The R3B is too low in concentration to aggregate itself. Aggregation in rhodamine dyes occurs at concentrations above $\sim3\times10^{-3}$ mol/L.[53] Detailed electronic absorption studies of the DMA from low concentrations to the highest concentration used in the experiments were performed. No change in the optical absorption was observed between low and high concentration, indicating that DMA is not aggregating. Aggregation does not account for the unusual experimental results observed in ethylene glycol.

Another question is whether deviations from the Marcus nonadiabatic rate can account for the data. It is possible that electron transfer is adiabatic near contact, where the electronic coupling is as strong as $(300\ \mathrm{cm}^{-1})^2$. Fits to the data were attempted with two different models for the electron transfer rate constant that include the changeover from nonadiabatic to adiabatic transfer as the electronic coupling increases.[54,55] For a range of solvent longitudinal relaxation times from 0.2–200 ps, fits to the ethanol, propylene glycol, and ethylene glycol data were unsuccessful. It is impossible to fit the shape of the time decays well when an adiabatic rate is included at short distances. In addition, for the best fits to the time decays, the fluorescence yield data fits are even worse than with a purely nonadiabatic rate, indicating that the adiabatic rate does not model the experiment well. $1/k(r)$ at contact is just under 1 ps, a moderate value that appears to be modeled well by the Marcus form of the nonadiabatic transfer rate.

VI. SOLUTE–SOLUTE RADIAL DISTRIBUTION FUNCTION IN ETHYLENE GLYCOL

In the various attempts to fit the electron transfer data in ethylene glycol, all the parameters were varied and a physically reasonable fit was not achieved. In two other solvents, the data were also inconsistent with the fits obtained for the five solvents discussed in Sec. IV. In solvent mixtures 50/50 ethylene glycol/ethanol and 41/59 glycerol/ethanol, values of $J_0=540$ and 660 cm^{-1}, respectively, were required to fit the data. However, the model used in all of the theoretical calculations is based on the assumption that the donor–acceptor (solute–solute) radial distribution function tracks the solvent's radial distribution function.[23] Within this assumption, varying the solvent diameter over a range of possible values for a single solvent molecule did not bring the data in ethylene glycol and theory into agreement.

By relaxing the assumption that the donor–acceptor radial distribution function tracks the single molecule ethylene glycol radial distribution function, it is possible to obtain good fits for the ethylene glycol data and data taken in the two other solvents. In the calculations, a very large effective solvent diameter σ is used to calculate $g(r)$ and $D(r)$. The very large σ ($\sim$17 Å) places a high concentration of acceptors near contact [see Fig. 2(A)]. This results in a large amount of short-time transfer, which depends on acceptors being nearby (see Fig. 3). In addition, the decrease in acceptor concentration at distance 1.5σ slows longer-time transfer. Using a large σ to calculate the effective $D(r)$ with slip boundary conditions causes the reduced near-contact diffusion to occur over a long distance [see Fig. 2(B)], bringing new acceptors into electron transfer range more slowly. The long distance reduction in the rate of diffusion helps fit the slower long-time component (see Fig. 3). Slip boundary conditions were used for ethylene glycol because they were found to be the best for modeling rotational behavior of a rhodamine solute molecule in ethylene glycol.[51] The ethylene glycol data with fits using a large effective solvent di-

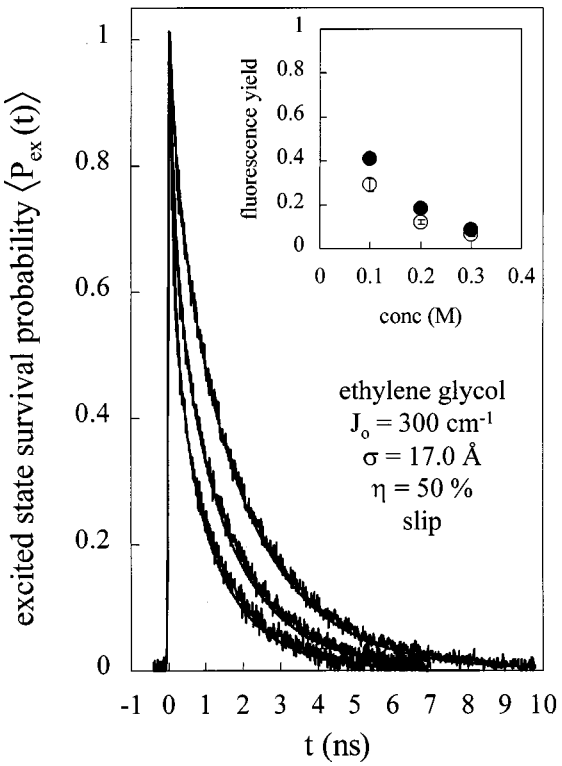

FIG. 8. R3B fluorescence data and fits for three concentrations of DMA in ethylene glycol. Inset shows fluorescence yield data (open circles) and fits (filled circles). Calculated curves use ethylene glycol parameters, $J_0 = 300\ \mathrm{cm}^{-1}$, $\beta = 1\ \text{Å}^{-1}$, and slip boundary conditions. However, an effective solvent diameter σ is varied and used in both the radial distribution function, $g(r)$, and the distance-dependent diffusion constant. Best fits to the time-dependent and fluorescence yield data are shown, with $\sigma = 17.0$ Å. The results demonstrate that the solutes do not track the solvent single molecule $g(r)$ in this strongly hydrogen bonding solvent.

ameter are shown in Fig. 8; $\sigma = 17$ Å and $\eta = 50\%$ are used to calculate $g(r)$ and $D(r)$.

Fits were also performed in which $\sigma = 17.0$ Å but $g(r) = 1$ after the first peak. The modified $g(r)$ was normalized to conserve concentration. However, curves calculated with this form of $g(r)$ were faster than the data at later times. It is only possible to fit the shape of the data if the dip after the first peak of $g(r)$ is also included. The decrease in acceptor concentration between the first and second solvent shells is necessary to get the experimentally observed slow transfer at later times.

It is also necessary to include a large σ in $D(r)$ calculations. Stick boundary conditions are not dependent on solvent diameter. However, given the large effective solvent diameter and the previous experiments that indicate slip boundary conditions are appropriate,[51] slip boundary conditions are used in the calculations. With slip boundary conditions, the solvent diameter plays a substantial role in determining $D(r)$. Making σ large in $g(r)$ is not sufficient to fit the data. It is not possible to fit the data with $\sigma = 4.34$ Å (the single molecule ethylene glycol diameter) in the hydrodynamic effect in Eq. (12). With a small σ, $D(r)$ reaches the bulk value, D, within a fairly short distance [see Fig. 2(B)]. Curves calculated with small values of σ in $D(r)$ are too fast at longer times, because acceptor molecules are diffusing in toward the donor too quickly. A large value of σ causes the bulk value of D to be reached only after a fairly long distance, which has the effect of slowing the long-time component of the electron transfer data. Using $\sigma \sim 17.0$ Å to calculate both $D(r)$ and $g(r)$ gives very good fits to the time and yield data.

The comparison of the electron transfer data in ethylene glycol to theory and the discussions given above in this section and in Sec. V strongly suggest that the donor–acceptor solute molecules in ethylene glycol are not following the single molecule solvent distribution function and are not diffusing in a manner consistent with a small molecule solvent. The system behaves as if the solutes are following the radial distribution function of enormous solvent molecules. Even though the hard sphere $g(r)$ does not model the single molecule ethylene glycol $g(r)$ perfectly, the ethylene glycol $g(r)$ will oscillate with a frequency associated with the ethylene glycol molecular diameter in a manner very similar to the calculated $g(r)$ used to describe the electron transfer.[52] It will not resemble a $g(r)$ calculated with $\sigma = 17.0$ Å.

Ethylene glycol can form multiple hydrogen bonds to yield a network-like structure.[45,52] One possible explanation for the large σ required to fit the data is that it represents an average ethylene glycol ''aggregate'' distance scale on which solute molecules are substantially precluded. In the theory, the aggregates are modeled as hard spheres. Clearly, hard spheres are not an accurate picture of the network structure that sets the distance scale for the solute distribution. Nonetheless, the hard sphere model seems to capture the essential features. Diffusion occurs among solvent aggregates of large size, consistent with slip boundary conditions. Slip boundary conditions are supported by the results of Moog *et al.* that show that solute rotation in ethylene glycol, glycerol, and ethylene glycol/glycerol mixtures is different from rotation in monoalcohols.[51] The fits to the data require the same $\sigma = 17$ Å in both $g(r)$ and $D(r)$. The fitting showed that it was necessary to have an oscillatory radial distribution function with the large σ. It was insufficient to have only a wide first peak in $g(r)$ and then a constant density. The donor–acceptor distance distribution appears to behave as if it is tracking a $g(r)$ with $\sigma = \sim 17$ Å.

Returning to Fig. 8, it can be seen that the model with $\sigma = 17$ Å and all other parameters fixed by the results from five other liquids (Sec. IV) can fit the data well but not perfectly. In particular, the yield at the lowest concentration has significant error. Using a model of large hard spheres rather than a more complex description of the solute distribution function may produce errors, particularly in the short-time and short-distance regimes. Yield calculations are very sensitive to such errors. In the lowest concentration ethylene glycol sample, more than 50% of the electron transfer occurs within the instrument response. At very short distances, the details of the distance distribution can play an important role in electron transfer dynamics. Because the donor–acceptor distance distribution function is modeled as hard sphere aggregates, it is reasonable to expect discrepancies. However, the only way to obtain anything near a reasonable fit with physically reasonable parameters is to use the large effective

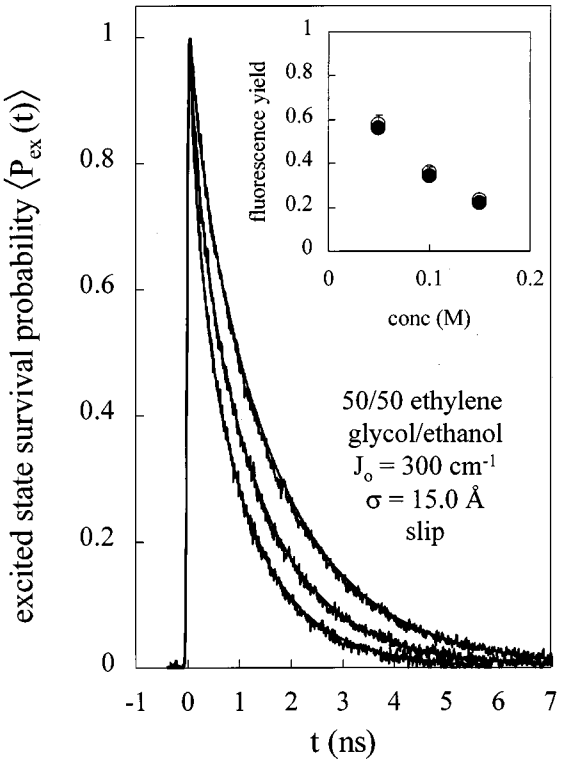

FIG. 9. R3B fluorescence data and fits for three concentrations of DMA in 50/50 v/v ethylene glycol/ethanol. Inset shows fluorescence yield data (open circles) and fits (filled circles). Calculated curves use ethylene glycol/ethanol parameters, $J_0 = 300\ cm^{-1}$, $\beta = 1\ Å^{-1}$, and slip boundary conditions. The effective solvent diameter σ was varied. Best fits to the time-dependent and fluorescence yield data are shown, with $\sigma = 15.0$ Å.

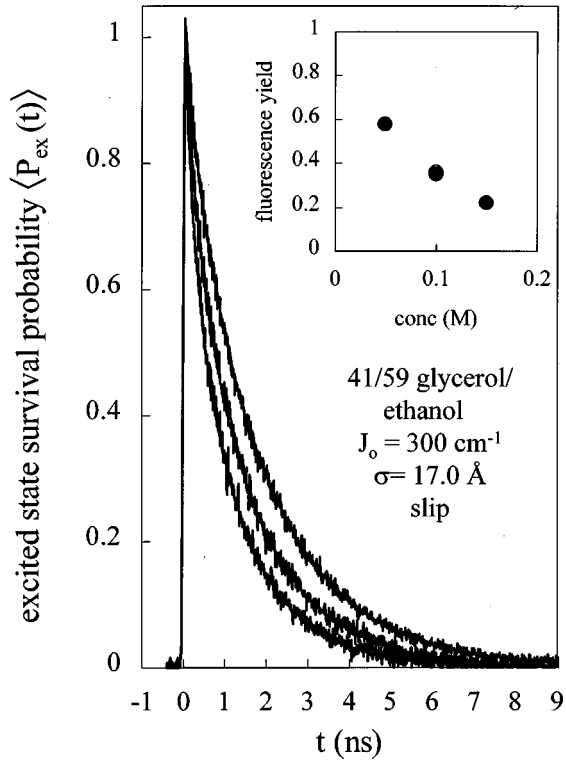

FIG. 10. R3B fluorescence data and fits for three concentrations of DMA in 41/59 v/v glycerol/ethanol. Inset shows fluorescence yield data (open circles) and fits (filled circles). Yield fits are so good that they completely obscure the data circles. Calculated curves use glycerol/ethanol parameters, $J_0 = 300\ cm^{-1}$, $\beta = 1\ Å^{-1}$, and slip boundary conditions. The effective solvent diameter σ was varied. Best fits to the time-dependent and fluorescence yield data are shown, with $\sigma = 17.0$ Å.

solvent diameter when calculating donor–acceptor distance distribution and hydrodynamic effect.

Another indication that the large effective solvent diameter provides a reasonable model of the solute–solute distribution function in ethylene glycol is the success of the model in fitting the data in two other solvents. Single parameter fits to J_0 resulted in $J_0 = 300 \pm 20\ cm^{-1}$ for five of the seven solvents originally studied (see Sec. IV and Figs. 4–6).[27] 50/50 ethylene glycol/ethanol and 41/59 glycerol/ethanol required J_0 values of approximately 600 cm^{-1}. This is well outside of the errors associated with the other fits. In addition, as in the electron transfer data taken in ethylene glycol, no physically reasonable choice of parameters can provide fits with $J_0 = 300\ cm^{-1}$. However, when J_0 is fixed at 300 cm^{-1} and σ is allowed to vary, very good fits to the data are obtained for these solvents. Again, the fits require a very large σ, and therefore, slip boundary conditions are appropriate although similar fits can also be obtained with stick boundary conditions. To fit the data requires $\sigma = 14$–19 Å. Data and fits are shown in Figs. 9 and 10. Ethylene glycol/ethanol fits were best with $\sigma = 15.0$ Å, and glycerol/ethanol fits were best with $\sigma = 17.0$ Å. In each case, these σ were used in both $g(r)$ and $D(r)$. Both the time-dependence and the yield fits are quite good.

Like ethylene glycol, 50/50 ethylene glycol/ethanol and 41/59 glycerol/ethanol require a large σ to obtain fits to the data that use electron transfer parameters that are consistent with the other five solvents. Table III may suggest an explanation for the differences between the five ''normal'' solvents and the three ''aggregated'' (large σ) solvents. The last three solvents in the table are the aggregated solvents. The first column of numbers is the mole percent of ethylene glycol or glycerol in each solvent. The second column of numbers is percent of the solvent's carbons that are bound to OH groups. The three solvents that display the aggregated behavior contain 36%, 51%, and 100% ethylene glycol or glycerol and have 73%, 76%, and 100% carbons with OH groups. The solvent 23/77 glycerol/2-butanol has 27 mole percent glycerol, but it acts as a normal solvent. Propylene glycol has 67% carbons with OH groups, but behaves as a normal solvent. The electron transfer data for propylene glycol is fit with stick boundary conditions. The data cannot be fit with slip boundary conditions, in accord with the solvent molecules being small compared to the solute molecules. The table suggests that to behave as an aggregated solvent, the solvent must have a very high percentage of carbons with OH groups and possibly must contain a substantial percentage of either ethylene glycol or glycerol. Pure ethylene glycol shows electron transfer behavior that deviates the most from a normal solvent. The data in this solvent cannot be fit at all with physically reasonable electron transfer parameters unless σ is very large. The other two aggregated solvents can be fit but the fitting parameter, J_0, can only be made to agree with the five normal solvents by using a large σ.

Ethylene glycol can form extended hydrogen bonding

networks.[45,52] The large effective solvent size modeled requiring a large σ in the $g(r)$ may arise from the difficulty of inserting solute molecules into the midst of such a network structure. The network structure interferes with solute molecules dispersing freely among the solvent molecules. The solutes, in some sense, occupy defect sites in the network. These sites that are more favorable for occupation by a solute occur on a distance scale that is large compared to the size of a single solute molecule. The solvents that have OH groups on 73% and 76% of their carbons and have substantial amounts of ethylene glycol or glycerol, molecules that have an OH bound to each carbon, may also have sufficient network character to behave in a manner that is similar to pure ethylene glycol. In contrast, propylene glycol, which has 67% of its carbons bound to an OH, is a normal liquid. Every propylene glycol molecule has a methyl group. In a propylene glycol hydrogen bonded network, the proximity of the methyls is each other in the network may provide the necessary defect sites, enabling the solutes to track the single molecule solvent radial distribution function.

The exact form of $g(r)$ used in the electron transfer calculation to model the solute–solute distribution in the aggregated solvents cannot be interpreted quantitatively because a simple hard sphere model was used and an appreciable amount of electron transfer occurs in these solvents at very short times (very short distances) that are beyond the time resolution of the experiments. However, important qualitative conclusions can be drawn from the results. The solute–solute distance distribution in the aggregated solvents must have a shell near contact with a very specific high concentration of acceptors and a shell farther out with an acceptor concentration much lower than the bulk concentration. Solute molecules distribute themselves in solution as if they were following the radial distribution function of large effective-solvent molecules created by hydrogen bonding networks. The same large effective-solvent size is necessary in both the $g(r)$ and the $D(r)$ to fit the data.

VII. CONCLUDING REMARKS

Intermolecular photoinduced donor–acceptor electron transfer is extremely sensitive to the spatial distribution of acceptors about a donor on a very short distance scale. Because of this fact, electron transfer can be used as a probe of spatial structure on the scale of angstroms. In this article, electron transfer data in ethylene glycol has been presented, analyzed, and compared to data presented previously.[27] It has been shown that an electronic coupling magnitude of $J_0 = 300\,\mathrm{cm}^{-1}$ fits data in eight solvents if the model that the donor–acceptor (solute–solute) distance distribution tracks the solvent radial distribution function[23] is modified for strongly hydrogen bonding solvents. The electron transfer data in ethylene glycol can only be fit if the single molecule radial distribution function is replaced with a radial distribution function in which an effective solvent size of $\sigma = 17$ Å is employed, although the diameters of the solvent molecules are only $\sigma \sim 4$–5 Å. It is necessary to use the large value of σ in both the radial distribution function and the hydrodynamic effect to obtain electron transfer parameters consistent with those from five normal solvents. It is suggested that solvent hydrogen bonding networks inhibit solute molecules from dispersing freely in ethylene glycol and two solvent mixtures containing ethylene glycol and glycerol. The hard sphere approach used to model the radial distribution must be considered approximate in modeling the solvent ''aggregates,'' but the results do provide a reasonable measure of the solute–solute spatial distribution.

Because a portion of the electron transfer is occurring within the instrument response of the time-dependent experiments, future experiments will be performed on apparatus with better time resolution. These experiments should provide more insight into the specifics of the short-time behavior, leading to a better understanding of electron transfer dynamics in solution and higher sensitivity to the exact nature of the solute–solvent interactions on a short distance scale.

ACKNOWLEDGMENTS

The authors would like to thank Professor Hans C. Andersen and Professor Vijay Pande, Department of Chemistry, Stanford University, for useful discussions on structure in hydrogen bonding solvents. We would like to thank Kristin Weidemaier for help performing preliminary experiments on this project and Maxim Kalashnikov for his participation in the experiments and analysis. This research was supported by the Department of Energy, Office of Basic Energy Sciences (Grant DE-FG03-84ER13251).

[1] D. Chandler, *Introduction to Modern Statistical Mechanics* (Oxford University Press, New York, 1987).
[2] L. Stryer, Annu. Rev. Biochem. **47**, 819 (1978).
[3] M. D. Ediger, R. P. Domingue, and M. D. Fayer, J. Chem. Phys. **80**, 1246 (1984).
[4] K. A. Peterson, M. B. Zimmt, S. Linse, R. P. Domingue, and M. D. Fayer, Macromolecules **20**, 168 (1987).
[5] N. Sutin, in *Electron Transfer in Inorganic, Organic, and Biological Systems*, edited by J. R. Bolton, N. Mataga, and G. McLendon (The American Chemical Society, Washington, DC, 1991), p. 25.
[6] M. R. Wasielewski, in *Photoinduced Electron Transfer. Part A: Conceptual Basis*, edited by M. A. Fox and M. Chanon (Elsevier, New York, 1988), p. 161.
[7] R. A. Marcus, J. Chem. Phys. **24**, 966 (1956).
[8] R. A. Marcus, J. Chem. Phys. **24**, 979 (1956).
[9] D. Rehm and A. Weller, Isr. J. Chem. **8**, 259 (1970).
[10] H. L. Tavernier, A. V. Barzykin, M. Tachiya, and M. D. Fayer, J. Phys. Chem. B **102**, 6078 (1998).
[11] H. L. Tavernier and M. D. Fayer, J. Phys. Chem. B **104**, 11541 (2000).
[12] L. Hammarström, T. Norrby, G. Stenhagen, J. Martensson, B. Akermark, and M. Almgren, J. Phys. Chem. B **101**, 7494 (1997).
[13] M. R. Arkin, E. D. A. Stemp, C. Turro, N. J. Turro, and J. K. Barton, J. Am. Chem. Soc. **118**, 2267 (1996).
[14] H. Shioyama, A. Takami, and N. Mataga, Bull. Chem. Soc. Jpn. **58**, 1029 (1985).
[15] M. Inokuti and F. Hirayama, J. Chem. Phys. **43**, 1978 (1965).
[16] M. Tachiya, Radiat. Phys. Chem. **21**, 167 (1983).
[17] J. R. Miller, J. V. Beitz, and R. K. Huddleston, J. Am. Chem. Soc. **106**, 5057 (1984).
[18] R. C. Dorfman and M. D. Fayer, J. Chem. Phys. **96**, 7410 (1992).
[19] S. F. Swallen, K. Weidemaier, and M. D. Fayer, J. Chem. Phys. **104**, 2976 (1996).
[20] S. F. Swallen, K. Weidemaier, H. L. Tavernier, and M. D. Fayer, J. Phys. Chem. **100**, 8106 (1996).
[21] R. A. Marcus, Annu. Rev. Phys. Chem. **15**, 155 (1964).
[22] R. A. Marcus and N. Sutin, Biochim. Biophys. Acta **811**, 265 (1985).
[23] G. J. Throop and R. J. Bearman, J. Chem. Phys. **42**, 2408 (1965).
[24] S. H. Northrup and J. T. Hynes, J. Chem. Phys. **71**, 871 (1979).
[25] J. M. Deutch and B. U. Felderhof, J. Chem. Phys. **59**, 1669 (1973).
[26] S. A. Rice, *Diffusion-Limited Reactions* (Elsevier, Amsterdam, 1985).

[27] H. L. Tavernier, M. M. Kalashnikov, and M. D. Fayer, J. Chem. Phys. **113**, 10191 (2000).
[28] K. Weidemaier, H. L. Tavernier, S. F. Swallen, and M. D. Fayer, J. Phys. Chem. A **101**, 1887 (1997).
[29] S. Murata, S. Y. Matsuzaki, and M. Tachiya, J. Phys. Chem. **99**, 5354 (1995).
[30] P. G. Wolynes and J. M. Deutch, J. Chem. Phys. **65**, 450 (1976).
[31] R. Zwanzig, Adv. Chem. Phys. **15**, 325 (1969).
[32] R. C. Dorfman, Y. Lin, and M. D. Fayer, J. Phys. Chem. **94**, 8007 (1990).
[33] Y. Lin, R. C. Dorfman, and M. D. Fayer, J. Chem. Phys. **90**, 159 (1989).
[34] J. R. Bolton and M. D. Archer, in *Electron Transfer in Inorganic, Organic, and Biological Systems*, edited by J. R. Bolton, N. Mataga, and G. McLendon (The American Chemical Society, Washington, DC, 1991), p. 7.
[35] H. B. Gray and J. R. Winkler, Annu. Rev. Biochem. **65**, 537 (1996).
[36] G. L. Closs and J. R. Miller, Science **240**, 440 (1988).
[37] J. M. Hale, in *Reactions of Molecules at Electrodes*, edited by N. S. Hush (Wiley Interscience, New York, 1971), p. 229.
[38] J. Y. Liu and J. R. Bolton, J. Phys. Chem. **96**, 1718 (1992).
[39] F. Markel, N. S. Ferris, I. R. Gould, and A. B. Myers, J. Am. Chem. Soc. **114**, 6208 (1992).
[40] M. Chanon, M. D. Hawley, and M. A. Fox, in *Photoinduced Electron Transfer. Part A: Conceptual Basis*, edited by M. A. Fox and M. Chanon (Elsevier, New York, 1988), p. 1.
[41] A. Weller, Z. Phys. Chem., Neue Folge **133**, 93 (1982).
[42] L. Verlet and J. J. Weis, Phys. Rev. A **5**, 939 (1972).
[43] J. P. Hansen and I. R. McDonald, *Theory of Simple Liquids* (Academic, London, 1976).
[44] D. A. McQuarrie, *Statistical Mechanics* (Harper & Row, New York, 1976).
[45] H. C. Andersen (private communication).
[46] J. K. Percus, Phys. Rev. Lett. **8**, 462 (1962).
[47] E. Thiele, J. Chem. Phys. **39**, 474 (1963).
[48] M. S. Wertheim, Phys. Rev. Lett. **10**, 321 (1963).
[49] J. K. Percus and G. Y. Yevick, Phys. Rev. **120**, 1 (1958).
[50] W. R. Smith and D. Henderson, Mol. Phys. **19**, 411 (1970).
[51] R. S. Moog, M. D. Ediger, S. G. Boxer, and M. D. Fayer, J. Phys. Chem. **86**, 4694 (1982).
[52] J. A. Padró, L. Saiz, and E. Guàrdia, J. Mol. Struct. **416**, 243 (1997).
[53] D. R. Lutz, K. A. Nelson, C. R. Gochanour, and M. D. Fayer, Chem. Phys. **58**, 325 (1981).
[54] I. Rips and J. Jortner, J. Chem. Phys. **87**, 6513 (1987).
[55] Z. Wang, J. Tang, and J. R. Norris, J. Chem. Phys. **97**, 7251 (1992).
[56] J. A. Riddick, W. B. Bunger, and T. K. Sakano, *Organic Solvents: Physical Properties and Methods of Purification*, 4th ed. (Wiley, New York, 1986).
[57] J. A. Riddick and W. B. Bunger, *Organic Solvents: Physical Properties and Methods of Purification*, 3rd ed. (Wiley, New York, 1970).